Solar-Terrestrial Physics. 2019. Vol. 5. Iss. 4. P. 74–80. DOI: 10.12737/stp-54201910. © 2019 V.A. Martines-Bedenko, V.A. Pilipenko, V.I. Zakharov, V.A. Grushin. Published by INFRA-M Academic Publishing House
Original Russian version: V.A. Martines-Bedenko, V.A. Pilipenko, V.I. Zakharov, V.A. Grushin, published in Solnechno-zemnaya fizika. 2019. Vol. 5. Iss. 4. P. 90–98. DOI: 10.12737/szf-54201910. © 2019 INFRA-M Academic Publishing House (Nauchno-Izdatelskii Tsentr INFRA-M)

INFLUENCE OF THE VONGFONG 2014 HURRICANE ON THE IONOSPHERE AND GEOMAGNETIC FIELD AS DETECTED BY SWARM SATELLITES: 2. GEOMAGNETIC DISTURBANCES

V.A. Martines-Bedenko
Institute of Physics of the Earth,
Moscow, Russia, lera_m0@mail.ru

V.A. Pilipenko
Institute of Physics of the Earth,
Moscow, Russia, pilipenko_va@mail.ru
Institute of Space Research,
Moscow, Russia, pilipenko_va@mail.ru

V.I. Zakharov
Lomonosov Moscow State University,
Moscow, Russia, zvi_555@list.ru
A.M. Obukhov Institute of Atmospheric Physics RAS,
Moscow, Russia, zvi_555@list.ru

V.A. Grushin
Institute of Space Research,
Moscow, Russia, vgrushin@iki.rssi.ru

Abstract. Strong meteorological disturbances in the atmosphere, accompanied by the generation of waves and turbulence, can affect ionospheric plasma and geomagnetic field. To search for these effects, we have analyzed electromagnetic measurement data from low-orbit Swarm satellites during flights over the typhoon Vongfong 2014. We have found that there are "magnetic ripples" in the upper ionosphere that are transverse to the main geomagnetic field fluctuations of small amplitude (0.5–1.5 nT) with a predominant period of about 10 s caused by small-scale field-aligned currents. Presumably, these quasi-periodic fluctuations are produced by the satellite's passage through the quasi-periodic ionospheric structure with a characteristic scale of ~70 km induced by the interaction of acoustic waves excited by the typhoon with the E layer of the ionosphere. In one of the flights over the typhoon, a burst of high-frequency noise (~0.3 Hz) was observed, which can be associated with the excitation of the ionospheric Alfvén resonator by atmospheric turbulence.

Keywords: tropical cyclone, ionosphere, geomagnetic field, acoustic waves, Swarm satellites, field-aligned current.

INTRODUCTION

Geophysical processes with large energy release in the lithosphere (earthquakes), atmosphere (typhoons, hurricanes, storms), magnetosphere (magnetic storms, substorms) occur in all geophysical shells. Severe meteorological disturbances accompanied by generation of acoustic gravity waves (AGW) and turbulence in the atmosphere can affect the ionosphere. Numerous ground-based experiments on continuous ionospheric sounding have revealed sinusoidal signals in the F layer during strong thunderstorms and hurricanes [Prasad et al., 1975; Raju et al., 1981; Huang et al., 1985]. In the last decade, the ground-based sounding instruments have been supplemented with total electron content (TEC) measurements from GPS signals [Polyakova, Perevalova, 2011; Nishioka et al., 2013]. Phase measurements between spaced radio paths satellite–receiver have found periodic acoustic oscillations with amplitudes of ~0.2 TECU (~2 % of the background TEC) [Shao, Lay, 2016].

Ionospheric disturbances generated by intense meteorological phenomena occurred in a narrow frequency band (3–5 mHz) corresponding to the infrasonic range, bounded from below by the Brunt-Väisälä frequency (the characteristic period 5–10 min). These observations demonstrated the presence of an effective acoustic channel between the lower atmosphere and the upper ionosphere. As the acoustic signal propagates upward in the vertically stratified atmosphere, its amplitude increases, but absorption increases too. The limiting height the acoustic signal reaches decreases with increasing frequency. As a result, from a wide spectrum of acoustic waves excited by hurricanes and thunderstorms only 1–4 min waves reach the upper atmosphere. In this case, the acoustic signal asymptotically takes the form of the nonlinear *N* wave whose parameters weakly depend on radiation conditions. The area of impact on the ionosphere due to wavefront spreading is wider than the characteristic size of the typhoon. An important role in acoustic radiation propagation may be played by atmospheric waveguides through which resonant waveguide modes can propagate over considerable distances.

Atmospheric processes can also affect the electromagnetic field of the ionosphere. A possible exposure pathway is associated with the ionospheric dynamo in the conductive E layer — drag of charged particles by ionospheric neutral component motions and the local generation of electric currents [Pokhotelov et al., 1995]. The exciting current system comprises field-aligned currents (along the geomagnetic field $\mathbf{B}_o$), which carry the disturbance into the upper ionosphere. The possibility of generating electric fields and field-aligned currents in the ionosphere by AGW has been shown in a number of theoretical studies [Surkov et al., 2004; Zettergren, Snively, 2013, 2015].

A rise in the electromagnetic noise level and plasma density in the ionosphere over typhoons and hurricanes has been detected by LEO satellites [Mikhailova et al., 2000; Isaev et al., 2002, 2010]. Measurements on board the satellite Cosmos-1809 (at a height of ~800 km) have revealed localized disturbances of the quasi-stationary electric field up to 25 mV/m and concomitant variations in the electron density N_e up to 6 % over regions with strong atmospheric disturbances [Sorokin et al., 2005].

Due to the high sensitivity of magnetometers on board the most advanced LEO satellites, effects of the generation of magnetic disturbances driven by AGW on conductive ionospheric plasma have been detected. Magnetic transverse fluctuations at middle latitudes on the night side may be caused by field-aligned currents generated by medium-scale traveling ionospheric disturbances (TIDs) [Park et al., 2015]. Using magnetic field data from the CHAMP satellite, Nakanishi et al. [2014] have found magnetic ripple at middle and low latitudes — low-amplitude fluctuations (from 1 to 5 nT) with a period of about several tens of seconds in a plane perpendicular to $\mathbf{B}_o$. These low-amplitude fluctuations differ from the magnetospheric pulsations Pc2–3 recorded by LEO satellites [Yagova et al., 2015] in the fact that they can be observed at any local time (although their amplitudes in the daytime are ~3 times higher than in the nighttime), and their occurrence and amplitudes do not depend on parameters of the solar wind and geomagnetic activity. In addition, at low latitudes geomagnetic pulsations Pc3 are of magnetospheric origin: they are generated by a fast magnetosonic wave propagating to Earth's surface and are seen in the magnetic field compression component (parallel to $\mathbf{B}_o$) [Pilipenko, Heilig, 2016]. The observed magnetic fluctuations might have been caused by the spatial structure of field-aligned currents generated by the dynamo, excited by acoustic waves propagating from the lower atmosphere to the ionosphere. Swarm satellites confirmed the presence of magnetic ripple with a characteristic period of about several tens of seconds, which was caused by small-scale field-aligned currents, in the upper ionosphere at middle and low latitudes [Aoyama et al., 2017]. A statistical analysis has shown that mean amplitudes of these magnetic fluctuations during typhoons are higher than under quiet weather conditions. Using Swarm data on the magnetic field, Iyemori et al. [2015] have confirmed that the magnetic ripple represents the spatial structure of small-scale field-aligned currents.

The observed effects raise, however, some doubts as to their reliability since the satellite passage in the right place in the favorable period (weak geomagnetic disturbance, absence of plasma bubbles, etc.) is an extremely rare event. Constant geomagnetic noise and magnetospheric pulsations complicate an unambiguous identification of such weak (of the order of thousandths of one percent of the geomagnetic field strength) magnetic disturbances. Even single events represent, therefore, an important addition to the picture of the atmosphere–ionosphere coupling during dynamic phenomena.

We have analyzed electromagnetic and plasma measurements made by Swarm satellites when they flew over the typhoon Vongfong 2014. In the first part of [Zakharov et al., 2019], the emphasis was on large-scale plasma disturbances and methods of identifying disturbances associated with the typhoon against the equatorial anomaly. In this part of this paper, we focus on magnetic disturbances.

DATA AND ANALYSIS

The Swarm mission includes three satellites (A, B, and C) located in two near-polar orbits. The A and C satellites move at a height of ~470 km close to each other in similar orbits, spaced by ~1.4° in longitude. The orbit of the B satellite is at a height of ~510 km and displaced by ~135° with respect to the A and C satellite orbits [http://directory.eoportal.org/web/eoportal/ satellite-missions/s/swarm]. In this paper, we have used magnetic field vector measurements with a frequency of 50 Hz [Friis-Christensen et al., 2008]. The magnetic field data has been converted into the local {X, Y, Z} coordinate system with the Z-axis, oriented along the magnetic field **B**, and the X-axis, directed to Earth in the plane of the geomagnetic meridian. Also on board the Swarm satellites, Langmuir probes recorded the plasma density (with a sampling frequency of 2 Hz). From the magnetic field data by means of high-pass filtering we removed the trend with a critical period of 30 s. The paper presents electron density (plasma density) variations along the orbit $n(t)=N_e(t)-\langle N_e\rangle$ [cm^{-3}], where $\langle N_e\rangle$ is the mean value for the interval of interest.

In the center of the typhoon there is a cylindrical region ~30 km in diameter, where the wind speed and pressure are minimum [Pokrovskaya, Sharkov, 2011] — typhoon eye. Around the eye there is a quasi-cylindrical eye wall ~75 km in radius, in which the wind speed is maximum (up to 100 m/s). The closer is the periphery of the typhoon, the lower is the wind speed, being as low as ~15 m/s at 500–000 km from the typhoon center. Data on the typhoon path includes positions of the eye of the typhoon and wind intensities throughout its lifetime, provided by Japan Meteorological Agency [http://www.jma.go.jp/jma/jma-eng/jma-center/rsmc-hp-pub-eg/besttrack.html]. The position of the typhoon center is given with a periodicity of 3 hrs; for intermediate moments we use linear interpolation.

In addition, we have used space meteorological images, taken by camera MODIS (Aqua Moderate Resolution Imaging Spectroradiometer) in the visible range, from NASA's Goddard Space Flight Center [https://ladsweb.modaps.eosdis.nasa.gov]. The vertical projection of the Swarm orbit is superimposed on the satellite images.

RESULTS

Consider the Vongfong typhoon (5th category on the Saffir-Simpson Hurricane Wind Scale [http://www.nhc.noaa.gov/aboutsshws.php]) moving in the Western Pacific Ocean from the equator to Japan in October 2014. The temporal dynamics of the wind speed in the Vongfong typhoon is shown in Figure 1. The typhoon developed in the Equatorial Pacific Ocean on October 2–14, 2014 (days 276–288).

The maximum wind speed exceeded 140 m/s. Planetary geomagnetic indices show that geomagnetic conditions during the typhoon were quiet: $K_p<4$, $|Dst|<40$ nT (Figure 1). This allows us to expect a low level of geomagnetic disturbances driven by space weather.

Although during the typhoon there were quite a few satellite passages over the typhoon, not all of them can be used to search for possible effects. At equatorial latitudes (mainly during dusk hours) there are characteristic phenomena — plasma bubbles [Park et al., 2009] and spread-F

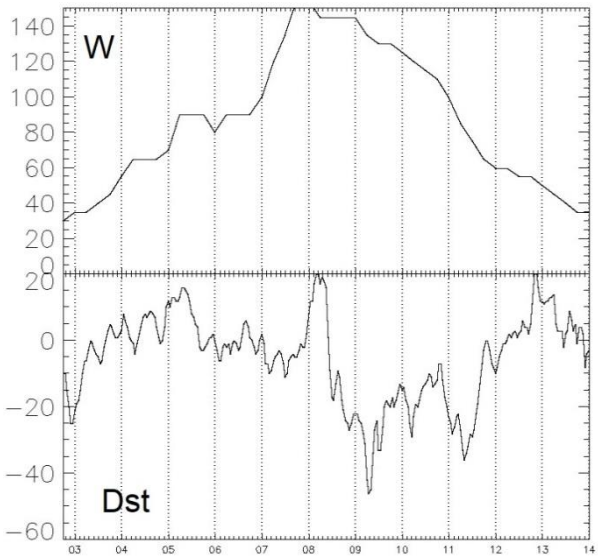

Figure 1. Temporal dynamics of wind speed *W* [m/s] in the Vongfong typhoon and geomagnetic index *Dst* [nT] on October 2–14, 2014 (days 276–288)

[Stolle et al., 2006], followed by geomagnetic fluctuations. We, therefore, ignore measurements made in the immediate vicinity of the geomagnetic equator (marked with the dashed red line on maps). At the same time, at higher middle latitudes the typhoon intensity decreases significantly. To isolate ionospheric effects of the typhoon in the ionosphere, we, therefore, consider low latitudes approximately from 10° to 30°.

The satellite passage directly over the geomagnetic equator is accompanied by fading of transverse magnetic fluctuations. This effect is caused by an almost horizontal orientation of the local geomagnetic field at which the excitation of Alfvén oscillations of field lines, completely immersed in the ionosphere, becomes impossible due to strong damping [Pilipenko et al., 1998].

October 8, 2014 (day 281)

At 01:18–01:23 UT, Swarm-A and -C passed directly over the typhoon during the daytime (LT~10). The wind speed during that period was as high as 140 m/s. The vertical projection of orbits of the satellites relative to the overall meteorological picture of the typhoon is depicted in Figure 2. The A and C satellites passed over the typhoon eye at 01:21 UT. The B satellite was in the nighttime sector (LT~23) and recorded an undisturbed magnetic field.

While passing over the typhoon, Swarm-A and -C recorded magnetic fluctuations with amplitudes x~1.5 nT, y~0.5 nT, z~0 (Figure 3). The dynamic spectrum (sonogram) of the x component shows that ~20 and ~7 s fluctuations prevail.

The absence of a disturbance in the z component suggests that the magnetic fluctuations were generated by field-aligned currents. The fluctuations recorded by Swarm-A and -C do not correlate.

Both the satellites recorded a plasma bubble with the electron density n~$8 \cdot 10^4$ cm^{-3} against the mean density $<N_e>=(1.0–2.5) \cdot 10^6$ cm^{-3} (see Figure 3, bottom panel). Thus, the relative magnitude of the plasma density perturbation is ~3–8 %. The time span of the bubble is ~80 s, which corresponds to the scale of spatial structure of ~ 560 km. This solitary plasma perturbation is interpreted in [Zakharov et al., 2019] as a result of the impact of the inner gravity wave on the upper ionosphere.

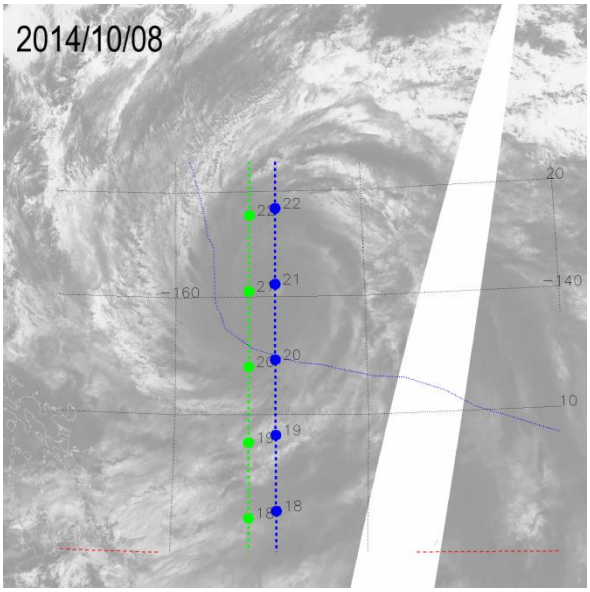

Figure 2. Passage of Swarm-A and -C over the typhoon on October 8, 2014, 01:17–01:23 UT (minutes are given near points on the orbit projection). The dashed red line indicates the geomagnetic equator. The thin blue line shows the trajectory of the typhoon, calculated from Japan Meteorological Agency data [http://www.jma.go.jp/jma/jma-eng/jma-center/rsmc-hp-pub-eg/besttrack.html]. Numbers near the points on trajectories of the satellites correspond to minutes in the plots of variations of the electron density and magnetic pulsations

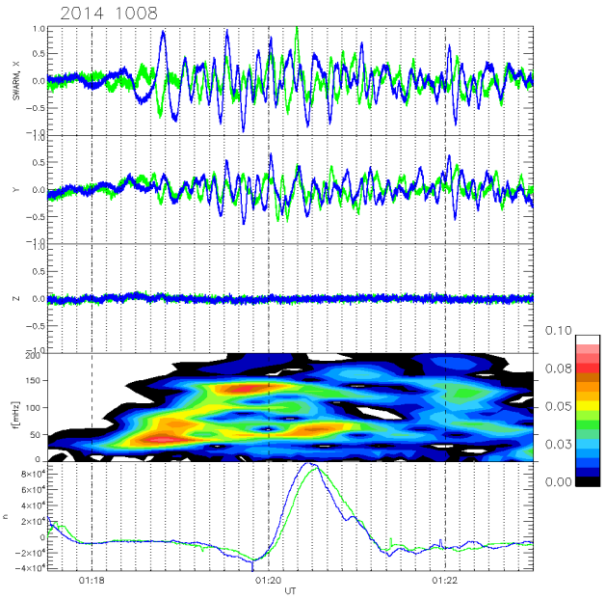

Figure 3. Geomagnetic field variations (three top panels: components *x*, *y*, *z* in the coordinate system (oriented by the current **B**), sonogram of the *x* component in the frequency range 0–200 mHz (panel 4) and electron density variations $n = N_e - <N_e>$ (bottom panel), recorded by Swarm-A (green line) and -C (blue line) on October 8, 2014, 01:17:30–01:23 UT. Time marks indicate every 10 s

In about an hour (02:06-02:11 UT), at ~11 LT, Swarm-B passed over the typhoon (over its eye at 02:09 UT) (see the projection of its orbit in the satellite image of the typhoon in Figure 4). When flying over the typhoon, Swarm-B recorded similar perturbations: plasma bubble with n~10^5 cm^{-3} and a burst of irregular magnetic oscillations only in transverse components with amplitudes x~1.0 nT, y~0.3 nT (Figure 5).

In all the cases, bursts of the intensity of geomagnetic fluctuations occur not only at the boundaries of the plasma bubble (where the maximum plasma density gradients are observed), but also in a wider area.

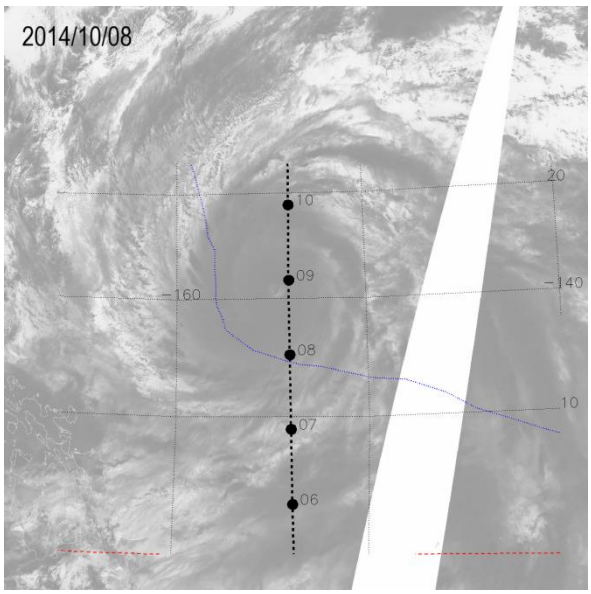

Figure 4. Passage of Swarm-B over the typhoon on October 8, 2014, 02:06–02:10 UT (notations are the same as in Figure 2)

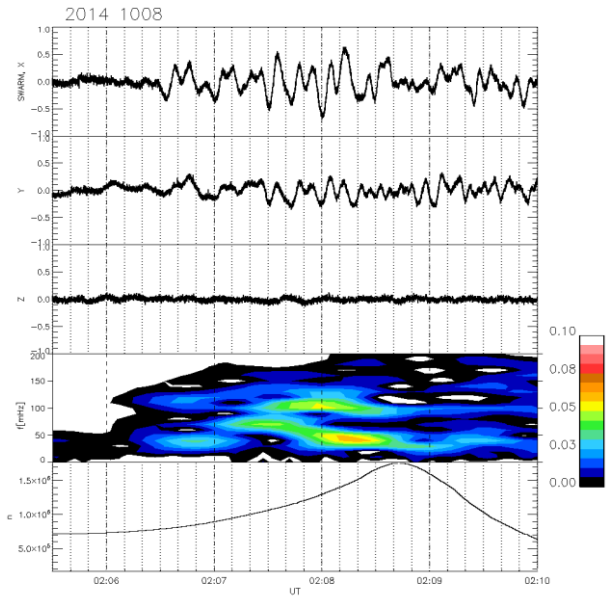

Figure 5. Geomagnetic field variations (three top panels: components x, y, z in the coordinate system (oriented by the current **B**), sonogram of the x component in a frequency range 0–200 mHz (panel 4), and electron density variations n (bottom panel), recorded by Swarm-B on October 8, 2014, 02:05:30–02:10 UT

October 8, 2014 (day 281)

The A and C satellites passed near the typhoon at 12:52–12:57 UT (at a latitude of its eye at 12:54 UT) at night (LT~22) (Figure 6). The wind speed during this period exceeded 130 m/s. There were no electron density perturbations at that time (Figure 7, bottom panel). Magnetometers of both the satellites detected a localized (duration of ~1 min) burst of quasi-periodic high-frequency perturbations in transverse components of the geomagnetic field (Figure 7).

The sonogram of the x component shows that in this event the burst of fluctuations occurred at a higher frequency of ~0.3 Hz. The amplitude of the magnetic fluctuations was low, x~0.4 nT.

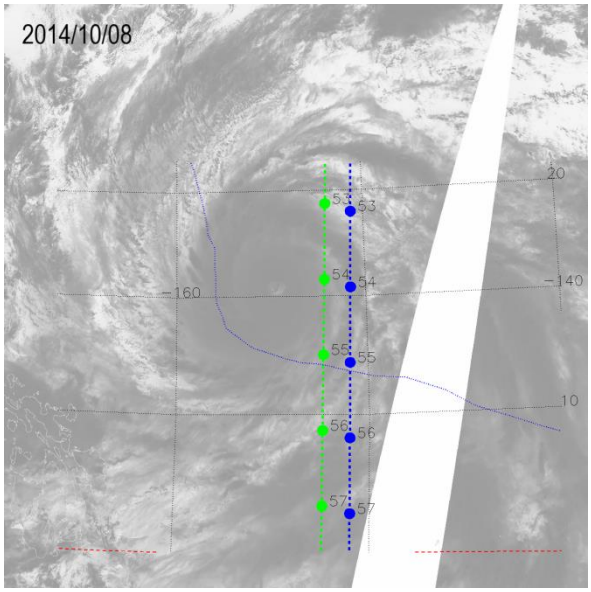

Figure 6. Passage of Swarm-A and -C over the typhoon on October 8, 12:52–12:58 UT (notations are the same as in Figure 2)

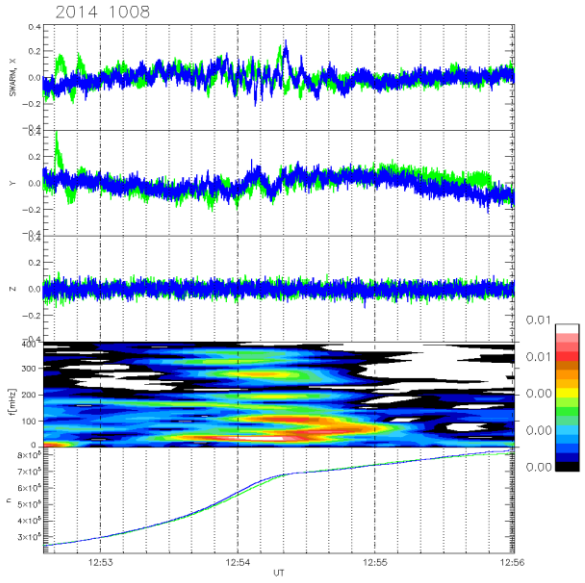

Figure 7. Geomagnetic field variations (three top panels: components x, y, z in the coordinate system (oriented by the current **B**), sonogram of the x component in a frequency range 0–400 mHz (panel 4) and electron density variations n (bottom panel), recorded by Swarm-A (green line) and -C (blue line) on October 8, 2014, 12:52:30–12:56 UT.

October 11, 2014 (day 284)

Swarm-A and -C passed over the typhoon at 01:19–01:24 UT (over its eye at 01:21 UT) (Figure 8). In the same period, Swarm-B passed ~10° to the east of Swarm-A and -C. The wind speed in the typhoon decreased to ~100 m/s.

During this period there were no electron density perturbations (Figure 9). Swarm magnetometers recorded an enhancement of magnetic noise — quasi-periodic high-frequency perturbations transverse to the geomagnetic field (Figure 9). The magnetic fluctuations reached the highest intensity at 01:21 UT. The quasi-periodic perturbations

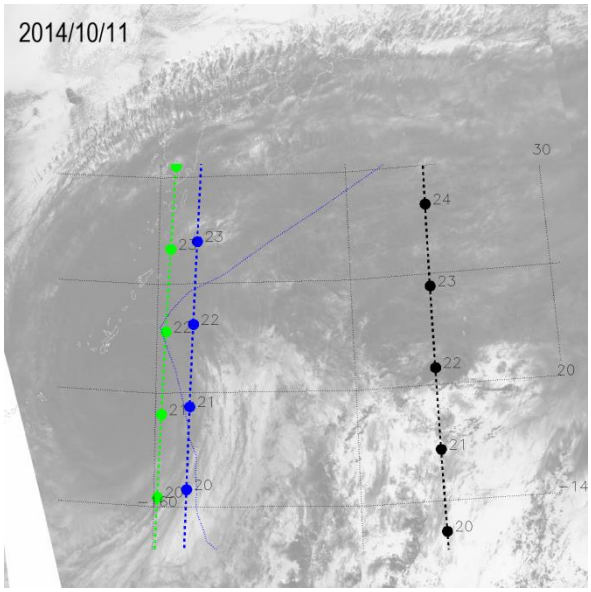

Figure 8. Passage of Swarm-A, -B, and -C over the typhoon on October 11, 2014, 01:18–01:22 UT (notations are the same as in Figure 2)

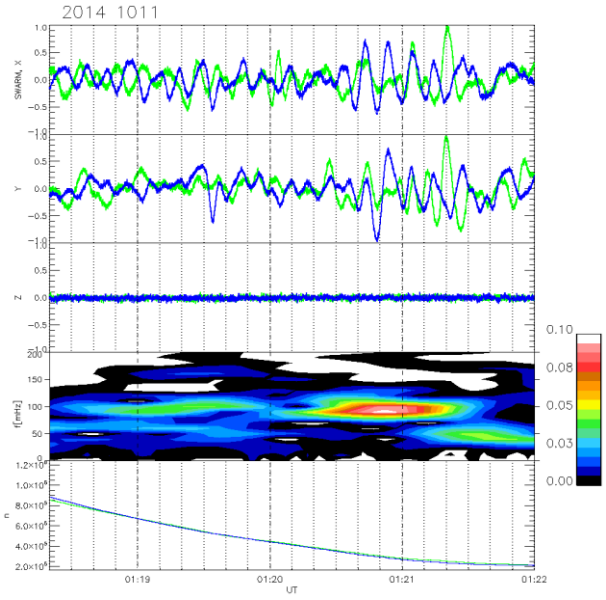

Figure 9. Geomagnetic field variations (three top panels: components *x*, *y*, *z* in the coordinate system (oriented by the current **B**), sonogram of the *x* component in a frequency range 0–200 mHz (panel 4) and electron density variations *n* (bottom panel), recorded by Swarm-A (green line) and -C (blue line) on October 11, 2014, 01:18:20–01:22 UT (in the same format as in Figure 3).

recorded by Swarm-A are incoherent with respect to those recorded by Swarm-C. The dynamic range of the *x* component shows that ~10 s fluctuations predominate.

Swarm-B whose orbit was away from the typhoon also detected magnetic field fluctuations in the frequency range considered, but their amplitude was several times lower (omitted in the paper).

DISCUSSION

Infrasonic acoustic waves can be excited in the typhoon both by winds and by powerful lightning discharges and intense sea disturbance (reaching 10 m). The high-frequency part (>10 mHz) of generated acoustic oscillations is absorbed in the upper atmosphere and is reflected from a sharp vertical temperature gradient at the lower edge of the ionosphere, and hence cannot be detected in the upper ionosphere. Generally, acoustic waves with frequencies 3–5 mHz can reach the conductive layer of the ionosphere (E layer) [Zettergren, Snively, 2015].

In the conductive layer of the ionosphere, the acoustic infrasonic oscillations generate electric fields and currents. The system of generated currents is divergent, and jets of the field-aligned current flow from the E layer to the upper ionosphere, where they can be detected by a satellite as geomagnetic field fluctuations. A possible minimum transverse scale of the disturbance is determined by diffusion spreading.

Irregular bursts of field-aligned currents, excited by the turbulence of the neutral atmosphere in the E layer, can resonantly intensify at frequencies of natural resonators: magnetospheric [Leonovich, Mazur, 1999] and ionospheric Alfvén resonator (IAR) [Surkov et al., 2004]. The fundamental period of IAR is of order of several seconds (frequency of about fractions of Hz), and that of the magnetospheric resonator at low latitudes is not shorter than 20–30 s [Pilipenko et al., 1998]. The events, we have analyzed, generally exhibited no enhancement of Alfvén oscillations with these periods over the typhoon. Only in the event shown in Figure 7 there was a burst of magnetic fluctuations with frequencies of ~0.3 Hz, which, in principle, can be attributed to IAR excitation.

There were largely bursts of transverse magnetic fluctuations with periods of ~10 s. The magnetic fluctuations reordered over the typhoon are similar in their properties to the magnetic ripple detected by CHAMP and Swarm [Nakanishi et al., 2014; Aoyama et al., 2017]. We also believe that these magnetic fluctuations result from the generation of field-aligned currents in the E layer of the ionosphere under the action of infrasonic oscillations excited by the typhoon. The horizontal scale of the acoustic wave does not exceed the wavelength $\lambda = C_s T$, where C_s is the sound velocity. For typical infrasonic periods T~4 min and the sound velocity C_s~0.3 km/s, λ~70 km. The passage of a satellite with V~7.5 km/s through an electromagnetic quasi-periodic structure of this scale will give variations with a period of <10 s, which falls within the range of the observed periods of the fluctuations.

Let us present a simple estimate by the order of magnitude of the excited magnetic field b in case of acoustic wave propagation through collisional plasma. In this medium, the Hall conductivity is

$$\sigma_H = \frac{eN}{B} R\left(\frac{\nu}{\Omega}\right),$$

where $R=(1+\nu^2/\Omega^2)^{-1}$, ν is the frequency of ion-neutral collisions, Ω is the ion cyclotron frequency. The neutral motion with V_n along the X-axis generates a drag current $j_x \cong eNV_n \sin\alpha R$. This transversal current in the conductive layer z_0 thick closes in on the field-aligned current,

$$j_\parallel = -\partial J_x / \partial x,$$

where J_x is the current integrated over the layer $J_x \cong j_x z_0$. The result is an estimated value of the field-aligned current produced by the acoustic wave:

$$j_\parallel \cong eNz_0 \sin\alpha R \partial V_n / \partial x.$$

The most intense field-aligned current jets occur in an acoustic wave front, where $\partial V_n/\partial x$ is large, especially if due to nonlinear distortions the front thickness is sufficiently small. The transverse current induced by the neutral motion in the conductive layer is channeled in a narrow region whose size is equal to the thickness of the acoustic wave front. For fluctuation with b~1 nT, $B=10^4$ nT at a wavefront 1 km thick, the related density of field-aligned current in the F layer should be j~1 μA/m^2.

Field-aligned current jets flowing from the E layer generate a relative magnetic disturbance in the upper ionosphere

$$\frac{b}{B} \cong \frac{\mu}{B}\int j_\parallel dx \cong \frac{V_n}{V_H}\sin\alpha.$$

Here, $V_H=(\mu_0\Sigma_H)^{-1}$ is the Hall ionospheric velocity determined by the E-layer height-integrated conductivity $\Sigma_H \cong \sigma_H z_0$ [S]. Assuming V_n~10 m/s, V_H~800/Σ_H~100 km/s, and sinα~0.2, we get $b/B \sim 0.2\cdot10^{-4}$. In the geomagnetic field, B~$5\cdot10^4$ nT, the disturbance is b~1 nT. This rough estimate agrees with magnitudes of the observed disturbances, thus confirming the reality of the mechanism discussed.

Bursts of 10 s geomagnetic fluctuations are observed in each passage of the Swarm satellites over the typhoon, but they are often short-term (3–4 periods). The geomagnetic fluctuations recorded by Swarm-A and -C are incoherent. This suggests that the scale of the disturbance is smaller than the distance between Swarm-C and -A, spaced longitudinally by ~1.4° (~160 km).

There were also events not related to the typhoon when the plasma bubble was accompanied by quasi-periodic (5–10 s) geomagnetic field fluctuations. This is due to the occurrence of equatorial plasma bubbles (or equatorial spread-F) at low latitudes during the dusk hours, representing flux tubes ~100 km wide with low plasma density (but with increased magnetic field strength due to the diamagnetic effect) [Luhr et al., 2002], which are generated at the bottom of the F layer, emerge upward, and spread to the north and south from the equator [Stolle et al., 2006]. The magnetic effect of the plasma bubbles (~0.5 nT) manifests itself, however, in the longitudinal component of the magnetic field, which cannot explain the effects we detected.

Due to the geomagnetic dynamo effect, the intense meteorological phenomena are, in fact, a generator of Pc2 irregular Alfvén waves, emitted to the upper ionosphere and the magnetosphere. These waves may affect the trapped particles of the inner radiation belt at low heights [Pokhotelov et al., 1999]. Such effects have been observed by Melioransky [2007].

CONCLUSION

The above phenomena are one of the special cases of multi-stage energy exchange between waves in the neutral atmosphere and ionospheric plasma and magnetic field disturbances. In particular, acoustic waves generated by the typhoon propagate to ionospheric heights, where due to the geomagnetic dynamo effect they excite jets of field-aligned currents and transverse geomagnetic disturbances. In the upper ionosphere at low latitudes when passing over the typhoon Vongfong (2014), the Swarm LEO satellites recorded spots of magnetic ripple (with scales from several hundreds to thousands of kilometers) — broadband low-amplitude fluctuations (0.5–1.5 nT) with the predominant period of ~10 s, which were generated by quasi-periodic field-aligned currents with a transverse scale of ~70 km. These currents are driven, presumably, by infrasonic waves emitted by the typhoon. In rare events, over the typhoon there was a burst of high-frequency noise (~ 0.3 Hz), which can be attributed to the excitation of IAR by atmospheric turbulence.

The Swarm data was provided by the European Space Agency [https://earth.esa.int/web/ guest/swarm/ data-access]. This work was supported by RFBR grants No. 18-05-00108 (MVA) and No. 19-05-00941 (ZVI), and state contracts with IKI (GVA) and IPE (PVA). We are grateful to the reviewers for helpful comments.

REFERENCES

Aoyama T., Iyemori T., Nakanishi K. Magnetic ripples observed by Swarm satellites and their enhancement during typhoon activity. *Earth, Planets Space.* 2017, vol. 69, p.89. DOI: 10.1186/s40623-017-0679-2.

Friis-Christensen E., Lühr H., Knudsen D., Haagmans R. Swarm — an Earth observation mission investigating geospace. *Advances Space Research*. 2008, vol. 41, pp. 210–216. DOI: 10.1016/j.asr.2006.10.008.

Huang Y-N., Cheng K., Chen S-W. On the detection of acoustic-gravity waves generated by typhoon by use of real time HF Doppler frequency shift sounding system. *Radio Sci.* 1985, vol. 20, pp. 897–906. DOI: 10.1029/RS020i004p00897.

Isaev N.V., Sorokin V.M., Chmyrev V.M., Serebryakova O.N. Ionospheric electric fields related to sea storms and typhoons. *Geomagnetism and Aeronomy*. 2002, vol. 42, no. 5, pp. 638–643.

Isaev N.V., Kostin V.M., Belyaev G.G., Ovcharenko O.Ya., Trushkina E.P. Disturbances of the topside ionosphere caused by typhoons. *Geomagnetism and Aeronomy*. 2010, vol. 50, iss. 2, pp. 243–255. DOI: 10.1134/S001679321002012X.

Iyemori T., Nakanishi K., Aoyama T., Yokoyama Y., Koyama Y., Lühr H. Confirmation of existence of the small-scale field-aligned currents in middle and low latitudes and an estimate of time scale of their temporal variation. *Geophys. Res. Lett*. 2015, vol. 42, pp. 22–28. DOI: 10.1002/2014GL062555.

Leonovich A.S., Mazur V.A. Standing Alfven waves in the magnetosphere from a localized monochromatic source. *J. Geophys. Res.* 1999. vol. 104, pp. 2411–2420. DOI: 10.1029/98JA02680.

Luhr H., Maus S., Rother M., Cooke D. First in-situ observation of night-time F region currents with the CHAMP satellite. *Geophys. Res. Lett.* 2002, vol. 29, iss.10, 1489. DOI: 10.1029/2001GL013845.

Melioransky A.S. *Vysypanie elektronov iz radiatsionnykh poyasov i koltsevogo toka pod vliyaniem izluchenii taifunov v severo-zapadnoi chasti Tikhogo okeana. Taifun "Maik" i moshchnyi tropicheskii shtorm "Nell"* [Electron precipitation from radiation belts and ring current under the effect of typhoon emissions in the north-western part of the Pacific Ocean. Typhoon Mike and powerful tropical storm Nell]. Preprint of Space Research Institute no. 2136. Moscow, 2007, 18 p.

Mikhailova G., Mikhailow Ya., Kapustina O. ULF-VLF electric fields in the external ionosphere over powerful typhoons in Pacific Ocean. *Int. J. Geomag. Aeronomy*. 2000, vol. 2, pp. 153–158.

Nakanishi K., Iyemori T., Taira K., Lühr H. Global and frequent appearance of small spatial scale field-aligned currents possibly driven by the lower atmospheric phenomena as observed by the CHAMP satellite in middle and low latitudes. *Earth Planets Space*. 2014, vol. 66, article number: 40. DOI: 10.1186/1880-5981-66-40.

Nishioka M., Tsugawa T., Kubota M., Ishii M. Concentric waves and short-period oscillations observed in the ionosphere after the 2013 Moore EF5 tornado. *Geophys. Res. Lett*. 2013, vol. 40, pp. 5581–5586. DOI: 10.1002/2013GL057963.

Park J., Lühr H., Stolle C., Rother M., Min K.W., Michaelis I. The characteristics of field-aligned currents associated with equatorial plasma bubbles as observed by the CHAMP satellite. *Ann. Geophys.* 2009, vol. 27, pp. 2685–2697. DOI: 10.5194/angeo-27-2685-2009.

Park J., Lühr H., Kervalishvili G., Rauberg J., Michaelis I., Stolle C., Kwak Y.-S. Nighttime magnetic field fluctuations in the topside ionosphere at midlatitudes and their relation to medium-scale traveling ionospheric disturbances: the spatial structure and scale sizes. *J. Geophys. Res.* 2015, vol. 120, pp. 6818–6830. DOI: 10.1002/2015JA021315.

Pilipenko V., Heilig B. ULF waves and transients in the topside ionosphere. *Low-Frequency Waves in Space Plasmas*. John Wiley & Sons, 2016, pp. 15–29. (Geophysical Monograph Ser., vol. 216). DOI: 10.1002/9781119055006.ch2.

Pilipenko V.A., Yumoto K., Fedorov E., Kurneva N., Menk F. Field line Alfven oscillations at low latitudes. *Mem. Fac. Sci. Kyushu Univ. Ser. D: Earth Planet. Sci.* 1998, vol. 30, no. 1, pp. 23–43.

Pokhotelov O.A., Parrot M., Pilipenko V.A., Fedorov E.N., Surkov V.V., Gladyshev V.A. Response of the ionosphere to natural and man-made acoustic sources. *Ann. Geophys.* 1995, vol. 13, pp. 1197–1210. DOI: 10.1007/ s00585-995-1197-2.

Pokhotelov O.A., Pilipenko V.A., Parrot M. Strong atmospheric disturbances as a possible origin of inner zone particle diffusion. *Ann. Geophys.* 1999, vol. 17, pp. 526–532. DOI: 10.1007/s00585-999-0526-2.

Pokrovskaya I.V., Sharkov E.A. Tropical cyclones and tropical disturbances of the World Ocean: chronology and evolution: version 4.1 (2006–2010). Moscow, Universitet Publ., 2011, 212 p.

Polyakova A.S., Perevalova N.P. Investigation into impact of tropical cyclones on the ionosphere using GPS sounding and NCEP/NCAR reanalysis data. *Adv. Space Res*. 2011, vol. 48, pp. 1196–1210. DOI: 10.1016/j.asr.2011.06.014.

Prasad S.S., Schneck L.J., Davies K. Ionospheric disturbances by severe tropospheric weather storms. *J. Atmos. Terr. Phys*. 1975, vol. 37, pp. 1357–1363. DOI: 10.1016/0021-9169(75)90128-2.

Raju D.G., Rao M.S., Rao B.M., Jogulu C., Rao C.P., Ramanadham R. Infrasonic oscillations in the F2 region associated with severe thunderstorms. *J. Geophys. Res*. 1981, vol. 86, pp. 5873–5880. DOI: 10.1029/ JA086iA07p05873.

Shao X.-M., Lay E.H. The origin of infrasonic ionosphere oscillations over tropospheric thunderstorms. *J. Geophys. Res*. 2016, vol. 121. DOI: 10.1029/2005JA011184.

Sorokin V.M., Isaev N.V., Yaschenko A.K., Chmyrev V.M., Hayakawa M. Strong DC electric field formation in the low latitude ionosphere over typhoons. *J. Atmos. Solar-Terr. Phys.* 2005, vol. 67, pp. 1269–1279. DOI: 10.1016/j.jastp.2005.06.014.

Stolle C., Lühr H., Rother M., Balasis G. Magnetic signatures of equatorial spread F as observed by the CHAMP satellite. *J. Geophys. Res*. 2006, vol. 111, A02304. DOI: 10.1029/2005JA011184.

Surkov V.V., Pokhotelov O.A., Parrot M., Fedorov E.N., Hayakawa M. Excitation of the ionospheric resonance cavity by neutral winds at middle latitudes. *Ann. Geophys.* 2004, vol. 22, pp. 2877–2889. DOI: 10.5194/angeo-22-2877-2004.

Yagova N., Heilig B., Fedorov E. Pc2-3 geomagnetic pulsations on the ground, in the ionosphere, and in the magnetosphere: MM100, CHAMP, and THEMIS observations. *Ann. Geophys*. 2015, vol. 33, pp. 117–128. DOI: 10.5194/angeo-33-117-2015.

Zakharov V.I., Pilipenko V.A., Grushin V.A., Khamidullin A.F. Impact of Typhoon Vongfong 2014 on the ionosphere and geomagnetic field according to Swarm satellite data: 1. Wave disturbances of ionospheric plasma. *Solar-Terrestrial Physics*. 2019, vol. 5, iss. 2, pp. 101–108. DOI: 10.12737/stp-52201914.

Zettergren M.D., Snively J.B. Ionospheric signatures of acoustic waves generated by transient tropospheric forcing. *Geophys. Res. Lett.* 2013, vol. 40, pp. 5345–5349. DOI: 10.1002/ 2013GL058018.

Zettergren M.D., Snively J.B. Ionospheric response to infrasonic-acoustic waves generated by natural hazard events. *J. Geophys. Res*. 2015, vol. 120, pp. 8002–8024. DOI: 10.1002/2015JA021116.

URL: http://directory.eoportal.org/web/eoportal/satellite-missions/s/swarm (accessed 20 May 2019).

URL: https://ladsweb.modaps.eosdis.nasa.gov (accessed 20 May 2019).

URL: http://www.nhc.noaa.gov/aboutsshws.php (accessed 20 May 2019).

URL: http://www.jma.go.jp/jma/jma-eng/jma-center/rsmc-hp-pub-eg/besttrack.html (accessed 20 May 2019).

URL: https://earth.esa.int/web/guest/swarm/data-access (accessed 20 May 2019).

How to cite this article

Martines-Bedenko V.A., Pilipenko V.A., Zakharov V.I., Grushin V.A. Influence of the Vongfong 2014 hurricane on the ionosphere and geomagnetic field as detected by SWARM satellites: 2. Geomagnetic disturbances. *Solar-Terrestrial Physics*. 2019. Vol. 5. Iss. 4. P. 74–80. DOI: 10.12737/stp-54201910.